

Supplementary Material for the dynamic structure factor in impurity-doped spin chains

Annabelle Bohrdt^{1,2}, Kevin Jägering¹, Sebastian Eggert¹, and Imke Schneider¹

¹Physics Department and Research Center OPTIMAS, University of Kaiserslautern, D-67663 Kaiserslautern, Germany

²Department of Physics and Institute for Advanced Study, Technical University of Munich, 85748 Garching, Germany

Abstract. Here we review the bosonization of the spin-1/2 xxz -chain and the derivation of correlation functions, which are used to derive the recursive approach used in the main paper. First the criterium for the validity of the bosonization approximation is determined by analyzing the individual energy levels as a function of length, energy, and anisotropy. We then consider open boundary conditions and provide analytical expressions for the integrations. The corrections to the resulting expressions for smaller $K = 0.7$ and $K = 0.6$ (i.e. larger Δ) are analyzed numerically. Periodic boundary conditions and the integrated spectral weights are also considered. Finally, details for the derivation of the averaging procedure are presented.

The goal of these notes is to review the bosonization and calculation of correlation functions for finite spin-1/2 xxz -chains

$$H = J \sum_i (S_i^x S_{i+1}^x + S_i^y S_{i+1}^y + \Delta S_i^z S_{i+1}^z) \quad (1)$$

with L sites and open or periodic boundary conditions. Using the correlation functions we want to calculate the dynamic structure factor at low frequencies and near the antiferromagnetic wave-vector $k \approx \pi$, which is given by

$$\begin{aligned} S(\omega, k) &= \frac{1}{L} \sum_{j, j'} e^{-ik(j-j')} \int_{-\infty}^{\infty} dt e^{i\omega t} \langle S_j^z(t) S_{j'}^z(0) \rangle \\ &= \Delta\omega \sum_{m \neq 0} S_L(\omega_m, k) \delta(\omega - \omega_m) \end{aligned} \quad (2)$$

where in the last line we have used the Lehmann representation using spectral weights

$$S_L(\omega_m, k) = \frac{2\pi}{\Delta\omega} |\langle \omega_m | S_k^z | 0 \rangle|^2 \quad (3)$$

at discrete energies $\omega_m = m\Delta\omega$ assuming that nearly degenerate states at the same energy are implicitly summed over.

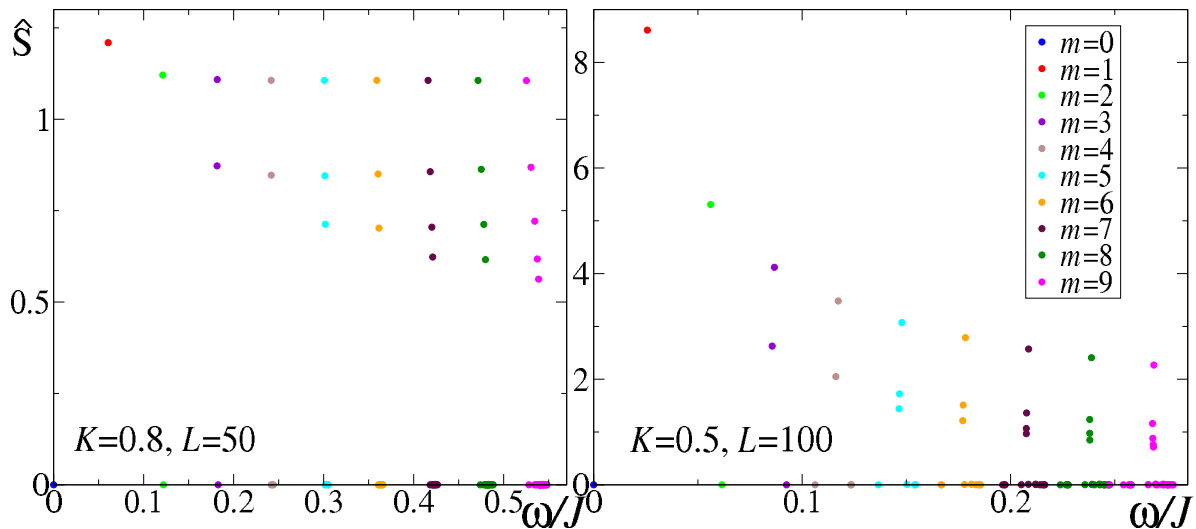


Figure 1. The total spectral weights \hat{S} for each individual state as a function of energy ω relative to the ground state energy for different L and K .

I. Validity of the bosonization approximation

For the derivation of bosonization in *finite* systems with open boundary conditions a strong assumption is usually made, that the spectrum can be described by a regularly spaced energy spectrum $\omega_m = m\Delta\omega$ with $\Delta\omega = \pi v/L$ and spinon velocity v [1], which is in fact implicitly required for Eq. (3). On the other hand it is known that this assumption never holds *exactly* in lattice systems. Cardy showed that energy levels will have finite size corrections of the form [2]

$$\omega_m = m \frac{\pi v}{L} \left(1 + c_m \left(\frac{\pi}{L} \right)^{d_n - 2} + \dots \right), \quad (4)$$

where d_n is the scaling dimension of the leading irrelevant operator. Moreover, each energy level does not correspond to a single state, but instead there is a whole set of nearly degenerate states, all of which may have slightly different energies due to the correction in Eq. (4). Unfortunately, the values of the correction coefficients c_m will in general be different for each of the nearly degenerate states and are not a priori known. For the spin-1/2 chain it is well known that there is a leading perturbing operator [3, 4, 5], which is expressed as the cosine of the bosonic field $\cos\sqrt{16\pi K}\phi$ and has scaling dimension $d_n = 4K$, but a systematic analysis of the region of validity where the corrections c_m in Eq. (4) can be neglected is so far missing as a function of L , m , and anisotropy K .

We therefore now present a short analysis of our numerical data in order to derive a reliable criterium for the regime where the corrections in Eq. (4) can be neglected. As an example we plot the total spectral weights \hat{S} in Fig. 1 for $K = 0.8$ and $L = 50$ as well as for $K = 0.5$ and $L = 100$. The grouping into nearly equally spaced energy levels labeled by m can clearly be seen as indicated by the different colors in Fig. 1.

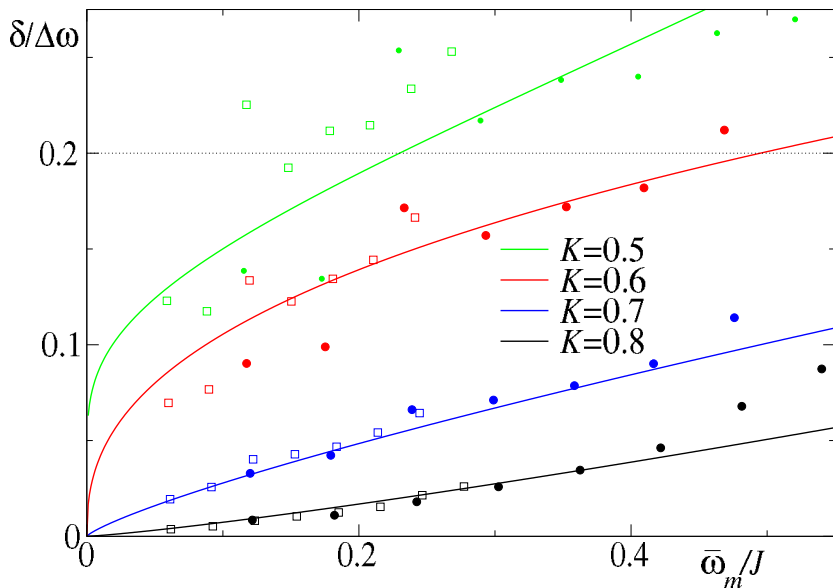


Figure 2. Relative standard deviation $\delta/\Delta\omega$ for the nearly degenerate energy levels as a function of mean energy $\bar{\omega}_m$ of the corresponding level in spin chains with different anisotropies K and length $L = 50$ (closed symbols) and $L = 100$ (open symbols). The lines for $K \geq 0.6$ are given by $0.4(\bar{\omega}_m/2.8J)^{4K-2}$ as a guide to the eye consistent with the powerlaw in Eq. (4). For the isotropic point $K = 0.5$ the line indicates logarithmic behavior $0.5/\ln(2.8J/\bar{\omega}_m)$.

The number of states in each level m increases quickly with the possible partitions of m , but only few states carry spectral weight [6], which can sometimes be explained by underlying symmetries [7].

The k -dependent spectral weight for each level m is implicitly summed up over the nearly degenerate states to obtain $S_L(\omega_m, k)$ in Eq. (3). This is justified for the levels in Fig. 1, since the energies of the states with non-zero spectral weights for a given m are very close, i.e. the energy spread is much smaller than the degeneracy lifting of other states and also can be assumed to be much smaller than the experimental resolution. However, in order to find a general condition for the validity of finite size bosonization, we require that *all* states for a given level m have a well defined energy separation to other states. For example in Fig. 1 for $L = 100$ and $K = 0.5$ we see that this condition still holds for $m = 7$, but levels $m = 8$ and $m = 9$ are not well separated any more. Note, however, that signal-carrying states with $\hat{S} \neq 0$ remain nearly degenerate in any case.

For a more comprehensive analysis we have determined the standard deviation δ of the energies for a large number of levels m at different lengths and anisotropies as a function of the mean energy $\bar{\omega}_m$ of the corresponding level as shown in Fig. 2 relative to the level spacing $\Delta\omega$. As a cutoff criteria of energetically separated levels we use $\delta/\Delta\omega < 0.2$ (dotted line), which is just below the value for $m = 7$, $L = 100$, and $K = 0.5$ in the example discussed above.

The deviation of each level in Fig. 2 increases with the index m , which is consistent

with a powerlaw m^{4K-2} . Together with the length behavior of the corrections in Eq. (4) with the same powerlaw $\Delta\omega^{4K-2} \propto (\pi/L)^{4K-2}$, this leads to a data collapse so that $\delta/\Delta\omega$ is only dependent on the mean energy $\bar{\omega}_m \approx m\Delta\omega$, which is well observed in Fig. 2 and valid for all lengths. In fact, the curves of $\delta/\Delta\omega$ for all anisotropies $K \geq 0.6$ approximately follow the same simple powerlaw $0.4(\bar{\omega}_m/2.8J)^{4K-2}$, while for the isotropic case $K = 0.5$ a logarithmic fit of the form $0.5/\ln(2.8J/\bar{\omega}_m)$ can be used.

In summary, we find a rather simple criteria for the bosonization predictions to hold which is independent of length, but simply requires that we are below an upper critical energy ω_c for each anisotropy K so that $\delta < 0.2\Delta\omega$. Numerically, we find from Fig. 2 $\omega_c(K = 0.5) \approx 0.2J$ and $\omega_c(K = 0.6) \approx 0.5J$. For even larger values of $K \geq 0.7$ (i.e. smaller Δ) the energy range is so large that we cannot determine a reliable cutoff from our numerics. The extrapolation curves would result in $\omega_c(K = 0.7) \approx 1.2J$ and $\omega_c(K = 0.8) \approx 1.6J$, but other non-linear effects are bound to become important around $\omega_c \sim 1J$ in any case.

II. Bosonization and correlations for open boundary conditions

The low-energy theory for the model in Eq. (1) is well described in the continuum limit by bosonic fields, which are rescaled by the square-root of the Luttinger parameter $K = \pi/2(\pi - \theta)$ where $\cos \theta = \Delta$ [3]. The free Hamiltonian is given by

$$H = \frac{v}{2} \int_0^L dx [\Pi(x)^2 + (\partial_x \phi(x))^2]. \quad (5)$$

where $v = J\pi \sin \theta/2\theta$ is the spinon velocity and Π is the momentum density conjugate to ϕ , $[\phi(x), \Pi(y)] = i\delta(x - y)$. Higher order corrections exist and are also interesting [1, 4, 5, 8], but can be neglected for low energies as quantitatively discussed in the previous section.

We are interested in the local S^z -operators, which can be expressed in terms of the bosons

$$S^z(x, t) = \sqrt{\frac{K}{\pi}} \partial_x \phi(x, t) + A(-1)^x \sin\left(\sqrt{4\pi K} \phi(x, t)\right), \quad (6)$$

where $A^2 = A_z/2$ is related to the amplitude of the asymptotic correlation functions, that is known from exact methods [9].

Open boundaries lead to the following mode expansion of the bosonic fields [1, 10]

$$\phi(x, t) = \hat{Q} \frac{2x}{L} + \phi_{\text{osc}}(x, t) \quad (7)$$

with

$$\phi_{\text{osc}}(x, t) = \sum_{\ell=1}^{\infty} \frac{1}{\sqrt{\pi\ell}} \sin \frac{\pi\ell x}{L} \left(e^{-i\frac{\pi\ell vt}{L}} b_{\ell} + e^{i\frac{\pi\ell vt}{L}} b_{\ell}^{\dagger} \right). \quad (8)$$

The zero mode \hat{Q} is given in terms of the total magnetization

$$S^z = \int_0^L \sqrt{\frac{K}{\pi}} \partial_x \phi = 2\sqrt{\frac{K}{\pi}} \hat{Q}. \quad (9)$$

Note that those expressions agree with previous works [3, 1, 10], up to an overall phase shift ϕ_0 in the boson, which is of no consequence.

For the dynamical structure factor near $k \approx \pi$ we are interested in the alternating part of the $S^z S^z$ -correlation function

$$\langle \sin(\sqrt{4\pi K}\phi(x, t)) \sin(\sqrt{4\pi K}\phi(y, 0)) \rangle = \frac{1}{2} (G^+(x, y, t) - G^-(x, y, t)) \quad (10)$$

with

$$G^\pm(x, y, t) = \langle e^{i2\pi S^z(x \mp y)/L} \rangle \langle e^{i\sqrt{4\pi K}\phi_{\text{osc}}(x, t)} e^{\mp\sqrt{4\pi K}\phi_{\text{osc}}(y, 0)} \rangle. \quad (11)$$

The first factor gives different results for even chains $S^z = 0$ and for odd chains $S^z = \pm 1/2$ [10]

$$\langle e^{i2\pi S^z(x \pm y)/L} \rangle = \begin{cases} 1, & L \text{ even} \\ \cos(\frac{\pi(x \pm y)}{L}), & L \text{ odd} \end{cases} \quad (12)$$

which reflects the different parity symmetry of the wavefunctions in even and odd chains. For the second factor in Eq. (11) it is useful to apply normal ordering

$$\exp\left(i\sqrt{4\pi K}\phi_{\text{osc}}(x, t)\right) = c(x) \exp\left(i\sum_{\ell} e^{i\omega_{\ell}t} \frac{A_{\ell}^{\dagger}(x)}{\sqrt{\ell}}\right) \exp\left(i\sum_{\ell} e^{-i\omega_{\ell}t} \frac{A_{\ell}(x)}{\sqrt{\ell}}\right) \quad (13)$$

where $\omega_{\ell} = \ell\Delta\omega$ with $\Delta\omega = \frac{\pi v}{L}$ and operators [11]

$$A_{\ell}(x) = 2\sqrt{K} \sin \frac{\pi\ell x}{L} b_{\ell}. \quad (14)$$

The prefactor is given via the Baker-Campbell-Hausdorff formula by

$$c(x) = \exp\left(-\sum_{\ell} \frac{2K}{\ell} \sin^2 \frac{\pi\ell x}{L}\right), \quad (15)$$

which is divergent. However, using

$$\sum_{\ell=1}^{\infty} q^{\ell}/\ell = -\log(1 - q) \quad (16)$$

it is possible to capture the dependence on L and x correctly, so that only an overall factor is dependent on the regularization, which we choose to be finite by setting

$$c(x) = \left(\frac{2L}{\pi} \sin \frac{\pi x}{L}\right)^{-K}. \quad (17)$$

Therefore, upon using Baker-Campbell-Hausdorff again, the correlation functions in Eq. (11) becomes

$$G^\pm(x, y, t) = c(x)c(y) \exp\left(\sum_{\ell=1}^{\infty} \frac{\pm 1}{\ell} e^{-i\omega_{\ell}t} \gamma_{\ell}(x, y)\right) \quad (18)$$

where we introduced the commutator

$$\gamma_\ell(x, y) = [A_\ell(x), A_\ell^\dagger(y)] = 4K \sin \frac{\ell\pi x}{L} \sin \frac{\ell\pi y}{L}. \quad (19)$$

For odd chains, the additional factor in Eq. (12) must also be inserted.

At this point all information for the large space-time behavior of the correlation function is known, which in fact can be expressed in closed form using Eq. (16) [1, 10, 12, 13]

$$G^\pm(x, y, t) = c(x)c(y) \left[\frac{\sin \frac{\pi(x+y-vt)}{2L} \sin \frac{\pi(x+y+vt)}{2L}}{\sin \frac{\pi(x-y-vt)}{2L} \sin \frac{\pi(x-y+vt)}{2L}} \right]^{\pm K} \quad (20)$$

for even L (and by including the factor in Eq. (12) for odd L). Note that we have normalized the correlation function so that

$$G^+(x, y, t) \rightarrow ((x-y)^2 - v^2t^2)^{-K} \quad (21)$$

in the thermodynamic limit away from the boundary. The overall prefactor must be determined from exact methods [9], so that the normalization in Eqs. (17) and (21) is simply a matter of convenience.

III. Fourier transform and recursive formula

To calculate the dynamical structure factor it is useful to go back to Eq. (18) in order to obtain the Fourier transformation in time. In accordance with the periodicity in t this yields an expansion in delta functions

$$\int_{-\infty}^{\infty} dt e^{i\omega t} G^\pm(x, y, t) = 2\pi \sum_m S_m^\pm(x, y) \delta(\omega - \omega_m). \quad (22)$$

where the discrete spectral weight for $\omega_m = m\Delta\omega = m\frac{\pi v}{L}$ is determined by the functions γ_ℓ in a recursive way [11],

$$S_m^\pm(x, y) = \frac{\pm 1}{m} \sum_{\ell=1}^m S_{m-\ell}^\pm(x, y) \gamma_\ell(x, y). \quad (23)$$

which simply follows from partial integration. This equation defines the recursion formula, which allows to calculate any individual spectral weight as a sum of the previous ones from starting values $S_0^\pm(x, y) = c(x)c(y)$ (and including Eq. (12) for odd L). Note that this is much easier than an integration over Eq. (20) which would require a small imaginary cutoff for the time and a complicated contour integration.

For the spatial Fourier transform we define

$$S_m^\pm(k) = \frac{1}{L} \int_0^L dx \int_0^L dy e^{i(\pi-k)(x-y)} S_m^\pm(x, y) \quad (24)$$

where the shift of the wavevector by π follows from the alternating factor in Eq. (6). Using $S_m(k) = \frac{A_z}{4} (S_m^+(k) - S_m^-(k))$ we obtain

$$S(\omega, k) = 2\pi \sum_m S_m(k) \delta(\omega - \omega_m). \quad (25)$$

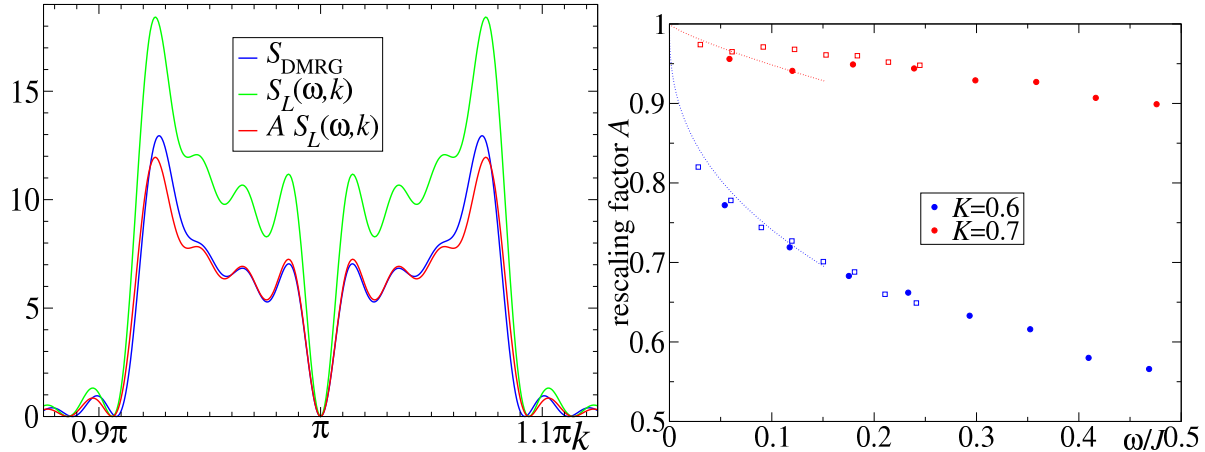


Figure 3. *Left:* The dynamical structure factor $S_L(\omega_m, k)$ for $K = 0.6$, $L = 100$ and $m = 8$ as a function of k from numerical DMRG calculations (blue) compared to bosonization (green) and rescaled bosonization predictions (red) using the prefactor $A = 0.649$. *Right:* The rescaling factor $A = S_{\text{DMRG}}/S_L^{\text{bosonization}}$ as a function of energy for different levels and lengths $L = 50$ (closed symbols) and $L = 100$ (open symbols). Lines are guides to the eye of the form $(1 - .26\omega^\gamma/\gamma)$ with $\gamma = 4K - 2$.

Since the integrand $S_m^\pm(x, y)$ in Eq. (24) only involves a sum of exponentials $\exp(i\ell_x\pi x/L)$ and $\exp(i\ell_y\pi y/L)$ according to Eqs. (23) and (19), it is possible to perform the integral for each such term analytically together with the prefactor $c(x)$ in Eq. (17) by using

$$\int_0^L dx \frac{e^{i\frac{\pi}{L}qx}}{(\sin \frac{\pi x}{L})^K} = \frac{\pi e^{i\pi q/2} 2^K L \csc(\pi K)}{\Gamma(K)\Gamma(q/2 - K/2 + 1)\Gamma(-q/2 - K/2 + 1)} \quad (26)$$

for $K < 1$ and analogously for the integration over y . In the summation of Eq. (23) we therefore keep track of the prefactors for each pair (ℓ_x, ℓ_y) for each level m and then add up the exactly known integrals as a function of k in Eq. (26) in the end. This implies that the expression of $S_L(\omega_m, k)$ for any energy and length is given as a closed *analytic* expression involving a simple finite sum over a large number of terms.

IV. Corrections for larger K

As shown in the paper the resulting expressions agree very well without any fitting parameter with numerical DMRG data for $K = 0.8$. On the other hand it is known that the corrections increase close to the isotropic point $\Delta \rightarrow 1$, i.e. $K \rightarrow 0.5$ as already discussed for the energies above. We have therefore analyzed the k -dependent spectral weights $S_L(\omega_m, k)$ also for $K = 0.6$ and 0.7 for different lengths using DMRG. A typical result for $K = 0.6$, $m = 8$ and $L = 100$ is shown in Fig. 3 (left). When using the normalization from Bethe ansatz, the bosonization gives a larger spectral weight (green), but after rescaling by a correction factor A the bosonization prediction (red) again coincides very well with the numerical data (blue). Therefore, we observe a rescaling

of the spectral weight, but surprisingly the momentum dependence is not strongly influenced by higher order corrections. For a further analysis we have determined the prefactors A for a large number of levels, anisotropies, and lengths and observe again a data collapse, so the rescaling is only a function of energy at each anisotropy K valid for all lengths as shown in Fig. 3 (right). The prefactor becomes significantly renormalized close to the isotropic point $K = 0.6$, but still approaches unity as $\omega \rightarrow 0$. Remarkably, such a correction factor can be trivially absorbed by the energy-dependent rescaling in Fig. 2 of the paper, while the k -dependence is quite accurately described by bosonization even for $K = 0.6$ (especially also the redistribution of spectral weights).

V. Periodic boundary conditions

The recursive approach is particularly simple for periodic boundary conditions. In this case the system is translationally invariant, so that $G^+(x, y, t)$ is a function of $x - y$ and t only and $G^-(x, y, t)$ vanishes. The prefactor is constant $c(x) = c = \left(\frac{2\pi}{L}\right)^K$. It is then convenient to introduce light-cone coordinates $z = vt - (x - y)$ and $\bar{z} = vt + x - y$ such that the correlation function factorizes with frequencies $u = \frac{1}{2}\left(\frac{\omega}{v} + k\right)$ and $\bar{u} = \frac{1}{2}\left(\frac{\omega}{v} - k\right)$

$$e^{-ik(x-y)} e^{i\omega t} G^+(x, y, t) = e^{iuz} e^{i\bar{u}\bar{z}} G(z) G(\bar{z}) \quad (27)$$

where k is measured relative to π and

$$G(z) = c \exp\left(\sum_{\ell} \frac{1}{\ell} e^{-i\frac{2\pi}{L}\ell z} \gamma\right) \quad (28)$$

with $\gamma = K$. The double Fourier transform in z and \bar{z} can then be performed directly by applying the recursion formula in Eq. (23) to the contributions of right-movers and left-movers separately. Due to periodicity with L in z and \bar{z} , the values for both u and \bar{u} are quantized

$$u = \frac{2\pi}{L} n \quad \bar{u} = \frac{2\pi}{L} \bar{n} \quad (29)$$

The boundaries of the integrals transform as follows:

$$\frac{1}{L} \int_0^L dx \int_0^L dy \rightarrow \frac{1}{L} \int_0^L dy \int_{-y}^{L-y} dr = \int_0^L dr \quad (30)$$

for integrands independent of y and L -periodic in r . Furthermore we use

$$\int_0^L dr \int_{-\infty}^{\infty} dt \rightarrow \frac{1}{2v} \int_{-\infty}^{\infty} dz \int_{-z}^{2L-z} d\bar{z} = \frac{1}{2v} \int_{-\infty}^{\infty} dz \int_0^{2L} d\bar{z} \quad (31)$$

for integrands invariant under $\bar{z} \rightarrow \bar{z} + L$. Since $\gamma = K$ is independent of ℓ in Eq. (28), the recursion can be solved exactly to give a ratio of gamma functions [11], i.e.

$$\int_{-\infty}^{\infty} e^{iuz} G(z) dz = \frac{2\pi c}{\Gamma(K)} \sum_n \frac{\Gamma(n+K)}{\Gamma(n+1)} \delta\left(u - \frac{2\pi}{L} n\right) \quad (32)$$

and

$$\int_0^{2L} e^{i\bar{u}\bar{z}} G(\bar{z}) d\bar{z} = \frac{2Lc}{\Gamma(K)} \sum_{\bar{n}} \frac{\Gamma(\bar{n}+K)}{\Gamma(\bar{n}+1)} \delta_{\bar{n}, \bar{u}L/2\pi} \quad (33)$$

for the integration over \bar{z} . Now using the exact result for the asymptotic amplitude of the alternating correlation functions A_z from Ref. [9] we obtain

$$S(\omega, k) = \frac{\pi A_z L c^2}{2v\Gamma^2(K)} \sum_{n, \bar{n}} \frac{\Gamma(n+K)}{\Gamma(n+1)} \frac{\Gamma(\bar{n}+K)}{\Gamma(\bar{n}+1)} \delta\left(u - \frac{2\pi}{L}n\right) \delta_{\bar{u}, 2\pi\bar{n}/L} \quad (34)$$

$$= \frac{\pi A_z L c^2}{2\Gamma^2(K)} \sum_m \sum_{l=-m}^m \frac{\Gamma(\frac{m+l}{2}+K)}{\Gamma(\frac{m+l}{2}+1)} \frac{\Gamma(\frac{m-l}{2}+K)}{\Gamma(\frac{m-l}{2}+1)} \delta\left(\omega - \frac{2\pi vm}{L}\right) \delta_{k, 2\pi l/L} \quad (35)$$

where the sum over l goes in steps of two, so that $l = n - \bar{n}$ and $m = n + \bar{n}$ are either both even or both odd and $|l| \leq m$. Comparing with Eq. (2) we can write for quantized frequencies $\omega_m = m\Delta\omega = m\frac{2\pi v}{L}$ and momenta $k_l - \pi = l\frac{2\pi}{L}$

$$S_L(\omega_m, k_l) = \frac{A_z L^2 c^2}{4v\Gamma^2(K)} \frac{\Gamma(\frac{m+l}{2}+K)}{\Gamma(\frac{m+l}{2}+1)} \frac{\Gamma(\frac{m-l}{2}+K)}{\Gamma(\frac{m-l}{2}+1)} \quad (36)$$

Stirling's formula for large arguments Λ gives

$$\frac{\Gamma(\Lambda+K)}{\Gamma(\Lambda+1)} \approx \Lambda^{K-1} \left(1 + \frac{K(K-1)}{2\Lambda} + \mathcal{O}\left(\frac{1}{\Lambda^2}\right)\right) \quad (37)$$

so that to leading order we find the bulk behavior in the thermodynamic limit

$$S_\infty(\omega, q + \pi) = \frac{\pi^2 A_z}{2v\Gamma^2(K)} 2^{2-2K} \left(\frac{\omega^2}{v^2} - q^2\right)^{K-1} \quad \text{for } v|q| < \omega, \quad (38)$$

where we get a factor of $1/2$ due to the fact that the quantization of k_l jumps in steps of two at a given m . The analogous analysis can be made for odd L where the prefactor in Eq. (12) basically gives the sum of two contribution with the k -quantization changed by one $l \rightarrow l \pm 1$.

VI. Integrated spectral weight

For the total spectral weight near the antiferromagnetic wave vector, we can integrate the contribution from the alternating correlation function

$$\widehat{S}(\omega) = \int dk S(\omega, k) \quad (39)$$

where the integral is taken in the vicinity of $k = \pi$. Let us also define the integrated spectral weight at discrete energies by

$$\widehat{S}(\omega) = 2\pi \sum_m \widehat{S}_m \delta(\omega - \omega_m). \quad (40)$$

with $\widehat{S}_m = \frac{A_z}{4} (\widehat{S}_m^+ - \widehat{S}_m^-)$. Integrating Eq. (24) over k generates a delta function $2\pi\delta(x-y)$ such that one spatial integration can be trivially performed and S_m simplifies to

$$\widehat{S}_m = \frac{\pi A_z}{2L} \int_0^L dx (S_m^+(x, x) - S_m^-(x, x)). \quad (41)$$

The functions $S_m^+(x, x)$ are generated recursively via Eq. (23). In case of periodic boundary conditions – since $\gamma_l(x, x) = 2K$ is independent of l – the recursion can again be solved exactly. From Eq. (32) we find

$$\widehat{S}_m = \frac{\pi A_z c^2}{2\Gamma(2K)} \frac{\Gamma(m + 2K)}{\Gamma(m + 1)}. \quad (42)$$

The bulk power law for the k -integrated structure factor is

$$\widehat{S}_\infty(\omega) = \frac{\pi^2 A_z}{v\Gamma(2K)} \left(\frac{\omega}{v}\right)^{2K-1}. \quad (43)$$

Note that this result can also be obtained by directly integrating Eq. (38).

VII. Averaging over chain lengths

For a doping density of $p = N_{imp}/N$ missing sites, the probability of finding a linear segment of length L is [14]

$$P(L) = p^2(1 - p)^L \approx p^2 \exp(-Lp), \quad (44)$$

which is normalized so $N \sum P(L) = N_{imp}$. The probability of a single site to belong to a segment of length L is $LP(L)$ which is normalized so that $N \sum LP(L) = N - N_{imp}$, which excludes the missing sites. In the limit of large chains or small doping, the sums can be converted to integrals since the signal does not change significantly as a function of length so that $\int dL P(L) = p$ and $\int dL LP(L) = 1$.

For a segment of length L we use the Lehmann representation in Eq. (2) in order to define the average signal

$$\bar{S}(\omega, k) = \sum_L P(L) L S(\omega, k) \approx \int dL P(L) \sum_m \pi v S_L(\omega_m, k) \delta(\omega - \omega_m) \quad (45)$$

which allows us to average separately over the bulk and impurity contributions in the $1/L$ expansion from the thermodynamic limit

$$S_L(\omega_m, k) \approx S_\infty(\omega_m, k) + \frac{1}{L} S_{\text{corr}}(\omega_m, k) + \mathcal{O}\left(\frac{1}{L^2}\right). \quad (46)$$

For the bulk average we find

$$\bar{S}_\infty = \int_0^\infty dL \pi v p^2 e^{-Lp} \sum_m S_\infty(\omega_m) \delta\left(\omega - m \frac{\pi v}{L}\right) \quad (47)$$

$$= \sum_m \int_0^\infty d\nu p^2 \frac{m \pi^2 v^2}{\nu^2} e^{-pm\pi v/\nu} S_\infty(\omega) \delta(\omega - \nu) \quad (48)$$

$$= \sum_m \frac{mp^2 \pi^2 v^2}{\omega^2} e^{-pm\pi v/\omega} S_\infty(\omega) \quad (49)$$

$$= E_1(\pi v p/\omega) S_\infty(\omega). \quad (50)$$

upon using the substitution $L = \frac{\pi v m}{\nu}$ and $dL = -d\nu \frac{m\pi v}{\nu^2}$. Here

$$E_1(y) = \sum_m m y^2 e^{-m y} = \frac{y^2 e^y}{(e^y - 1)^2} \quad (51)$$

is the Einstein function of the scaling variable $y = p\pi v/\omega$ which measures the "average-length" gap $v\pi/\bar{L}$ compared to ω [15, 16]. For the average impurity correction we use the same substitution $L = \frac{\pi v m}{\nu}$ and $dL = -d\nu \frac{m\pi v}{\nu^2}$

$$\bar{S}_{\text{imp}} = \int_0^\infty dL \frac{\pi v p^2 e^{-Lp}}{L} \sum_m S_{\text{imp}}(\omega_m) \delta\left(\omega - m \frac{\pi v}{L}\right) \quad (52)$$

$$= \sum_m \int_0^\infty d\nu p^2 \frac{\pi v}{\nu} e^{-p m \pi v / \nu} S_{\text{imp}}(\omega) \delta(\omega - \nu) \quad (53)$$

$$= \sum_m \frac{p^2 \pi v}{\omega} e^{-p m \pi v / \omega} S_{\text{imp}}(\omega) \quad (54)$$

$$= p E_2(\pi v p / \omega) S_{\text{imp}}(\omega). \quad (55)$$

which is proportional to p and the scaling function

$$E_2(y) = \sum_m y e^{-m y} = \frac{y}{e^y - 1}. \quad (56)$$

- [1] S. Eggert and I. Affleck, Magnetic impurities in half-integer Heisenberg antiferromagnetic chains, *Phys. Rev. B* **46**, 10866 (1992).
- [2] J.L. Cardy, Operator content of two-dimensional conformally invariant theories, *Nucl. Phys.* **B270**, 186 (1986).
- [3] For a review on bosonization see: T. Giamarchi, *Quantum Physics in One Dimension*, Oxford Univ. Press (Oxford 2003).
- [4] I. Affleck, D. Gepner, H.J. Schulz and T. Ziman, Critical behaviour of spin-s Heisenberg antiferromagnetic chains: analytic and numerical results, *J. Phys. A: Math. Gen.*, **22**, 4725 (1990).
- [5] J. Sirker and M. Bortz, The open XXZ-chain: Bosonisation, Bethe ansatz and logarithmic corrections, *J. Stat. Mech.* P01007 (2006).
- [6] I. Schneider, A. Struck, M. Bortz and S. Eggert, Local density of states for individual energy levels in finite quantum wires, *Phys. Rev. Lett.* **101**, 206401 (2008)
- [7] S.A. Söffing, I. Schneider, and S. Eggert Low-energy local density of states of the 1D Hubbard model *Europhys. Lett.* **101**, 56006 (2013).
- [8] M. Bortz, M. Karbach, I. Schneider, and S. Eggert, Lattice vs. continuum theory of the periodic Heisenberg chain, *Phys. Rev. B* **79**, 245414 (2009).
- [9] S. Lukyanov and V. Terras, Long-distance asymptotics of spin-spin correlation functions for the XXZ spin chain, *Nucl. Phys. B* **654**, 323 (2003).
- [10] S. Eggert, I. Affleck, and M. D. P. Horton, Néel order in doped quasi one-dimensional antiferromagnets, *Phys. Rev. Lett.* **89**, 047202 (2002).
- [11] I. Schneider and S. Eggert, Recursive method for the density of states in one dimension, *Phys. Rev. Lett.* **104**, 036402 (2010).
- [12] S. Eggert and I. Affleck, Impurities in S=1/2 Heisenberg antiferromagnetic chains: Consequences for neutron scattering and Knight shift, *Phys. Rev. Lett.* **75**, 934 (1995)
- [13] A.E. Mattsson, S. Eggert, and H. Johannesson, Properties of a Luttinger liquid with boundaries at finite temperature and size, *Phys. Rev. B* **56**, 15615 (1997).

- [14] S. Wessel and S. Haas, Excitation spectra and thermodynamic response of segmented Heisenberg spin chains, *Phys. Rev. B* **61**, 15262 (2000).
- [15] G. Simutis, *et al.*, Spin pseudogap in Ni-doped SrCuO₂, *Phys. Rev. Lett.* **111**, 067204 (2013).
- [16] G. Simutis, *et al.*, Spin pseudogap in the S=1/2 chain material Sr₂CuO₃ with impurities, *Phys. Rev. B* **95**, 054409 (2017).